Comparative Ten-vertex Metallaborane Chemistry: Some *nido*-6-Metalladecaboranes of Tungsten, Rhenium, Ruthenium, Osmium, and Iridium; including the Crystal and Molecular Structures of [6,6,6,6,6-$(PMe_2Ph)_3H_2$-*nido*-6-WB_9H_{13}] and [6,6,6-$(PMe_2Ph)_3$-*nido*-6-OsB_9H_{13}] *

Michael A. Beckett, Norman N. Greenwood, John D. Kennedy, and Mark Thornton-Pett
Department of Inorganic and Structural Chemistry, University of Leeds, Leeds LS2 9JT

Reaction of $[WH_6(PMe_2Ph)_3]$ with $[NEt_4][B_9H_{14}]$ yields the first wolfraborane, [6,6,6,6,6-$(PMe_2Ph)_3H_2$-*nido*-6-WB_9H_{13}]; the halcyon-blue air-stable compound has been characterised by a single-crystal *X*-ray diffraction analysis and by n.m.r. spectroscopy. Crystals are monoclinic, space group $P2_1/n$, with a = 1 571.7(5), b = 1 049.1(5), c = 1 961.5(8) pm, β = 94.30(3)°, and Z = 4. The molecular structure closely resembles that of *nido*-$B_{10}H_{14}$ with the BH unit at position 6 being subrogated by a $WH_2(PMe_2Ph)_3$ metal centre. In solution the compound exhibits fluxionality of the five *exo*-polyhedral ligands $(PMe_2Ph)_3H_2$ on the metal centre. Reaction of *mer*-$[OsCl_3(PMe_2Ph)_3]$ with $[NBu_4][B_9H_{14}]$ yields the new red air-stable osmaborane [6,6,6-$(PMe_2Ph)_3$-*nido*-6-OsB_9H_{13}] which has also been characterized by a single-crystal *X*-ray diffraction analysis and n.m.r. spectroscopy. Crystals are monoclinic, space group $P2_1/c$, with a = 957.8(1), b = 1 990.0(4), c = 1 671.4(3) pm, β = 94.01(1)° and Z = 4. The structure comprises *nido*-decaborane-like molecules in which the 6-BH unit has been subrogated by the isolobal $Os(PMe_2Ph)_3$ unit. The analogous reaction with *mer*-$[RuCl_3(PMe_2Ph)_3]$ yields the new dark amber ruthenaborane [6,6,6-$(PMe_2Ph)_3$-*nido*-6-RuB_9H_{13}], and with $[ReH_5(PMe_2Ph)_3]$ and $[NEt_4][B_9H_{14}]$ the previously reported rhenaborane [6,6,6,6-$(PMe_2Ph)_3H$-*nido*-6-ReB_9H_{13}] is formed in an improved yield of 65%. The new tungsten and osmium species together with the known *nido*-6-metalladecaboranes $[(PMe_2Ph)_3HReB_9H_{13}]$ and $[(PR_3)_2HIrB_9H_{13}]$ (R = Me or Ph) permit the structural and n.m.r. comparison of the metallaboranes across four adjacent groups of the Periodic Table; the systematic variation of the *exo*-polyhedral metal ligands across the sequence $WH_2(PMe_2Ph)_3$, $ReH(PMe_2Ph)_3$, $Os(PMe_2Ph)_3$, $IrH(PR_3)_2$ implies that each 18-electron metal centre is a three-orbital two-electron contributor to the cluster bonding, just like 6-BH in the structural parent *nido*-$B_{10}H_{14}$. For the compounds studied there is a progressive diminution of *ca.* 5 pm per elemental step in both the M–B and M–P interatomic distances across the series W, Re, Os, Ir, but the ^{11}B and ^1H n.m.r. properties indicate that the cluster bonding retains essentially *nido*-decaborane-like behaviour throughout.

Over 500 polyhedral metallaboranes have now been characterized and definitive structural work by diffraction methods has been carried out on about 100 of these involving some 40 different metals.[1-3] Despite this, comparative structural data and other behavioural trends across Periods or down Groups of the Periodic Table for particular polyhedral structural classes are surprisingly limited. It is of considerable interest to examine such trends and limits to stable metal-to-borane bonding within the known structural classes and, accordingly, we here report results for the ten-vertex 6-MB_9 system based on *nido*-$B_{10}H_{14}$. The metals involved are the four adjacent third-row transition elements tungsten, rhenium, osmium, and iridium, and the *exo*-polyhedral ligands co-ordinated to the metals have been restricted to varying numbers of PMe_2Ph and H so as to maintain a reasonably constant metal-bonding environment to aid the intercomparison. (We have noted in previous work[4-6] that interchange of phosphine and hydride ligands in metallaborane clusters produces surprisingly little change in cluster electronic structure as judged, for example, by changes in cluster boron-11 n.m.r. chemical shifts.) This approach has led to the synthesis of the new *nido*-6-metalladecaboranes $[(PMe_2Ph)_3H_2WB_9H_{13}]$ and $[(PMe_2Ph)_3OsB_9H_{13}]$ for comparison with the previously reported compounds $[(PMe_2Ph)_3HReB_9H_{13}]$[7] and $[(PPh_3)_2HIrB_9H_{13}]$.[8]

Results and Discussion

The wolfraborane [6,6,6,6,6-$(PMe_2Ph)_3H_2$-*nido*-6-WB_9H_{13}] (**1**) was obtained as a bright halcyon-blue microcrystalline powder in 21% yield by the direct reaction of $[WH_6(PMe_2Ph)_3]$ with the *arachno*-$[B_9H_{14}]^-$ anion in methylene chloride at room temperature. An identical procedure using $[ReH_5(PMe_2Ph)_3]$ as the starting metal complex gave the previously reported[7] compound [6,6,6,6-$(PMe_2Ph)_3H$-*nido*-ReB_9H_{13}] (**2**) as a purple microcrystalline solid in much improved yield (*ca.* 65%). Compound (**1**) was characterised by multielement n.m.r. spectroscopy (see later) and by a single-crystal *X*-ray diffraction analysis. The *nido*-cluster molecular structure is shown in Figure 1; the positions of the two terminal H and two bridging H atoms on the tungsten were not located. Selected interatomic distances and angles are in Tables 1 and 2. It can be seen that the structure closely resembles that of *nido*-$B_{10}H_{14}$[9] and individual distortions are slight. The retention of the diagnostically long *nido*-decaboranyl distances B(5)–B(10) and B(7)–B(8) is particularly noteworthy. In view of these structural parallels, the

* *nido*-6,6-Dihydrido-6,6,6-tris(dimethylphenylphosphine)-6-wolfradecaborane and *nido*-6,6,6-tris(dimethylphenylphosphine)-6-osmadecaborane respectively.

Supplementary data available (No. SUP 56444, 6 pp.): thermal parameters, H-atom co-ordinates. See Instructions for Authors, *J. Chem. Soc., Dalton Trans.*, 1986, Issue 1, pp. xvii—xx. Structure factors are available from the editorial office.

Non-S.I. unit employed: mmHg ≈ 133 N m^{-2}.

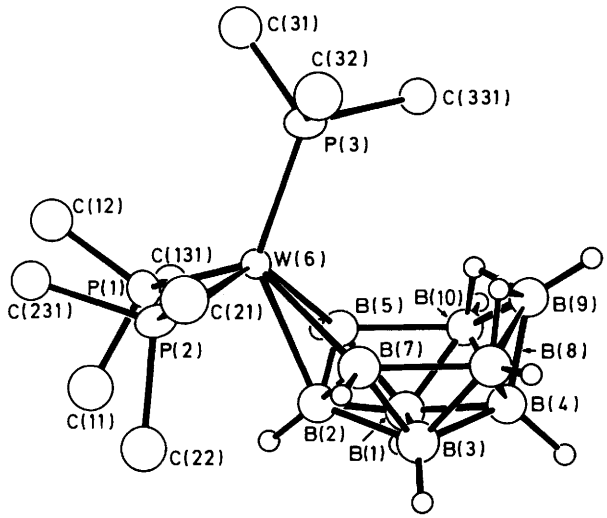

Figure 1. Molecular structure of $[(PMe_2Ph)_3H_2WB_9H_{13}]$ (**1**) with selected P-organyl group atoms omitted for clarity. All hydrogen atoms except those bound to W(6) were crystallographically determined. The distribution of two-electron bonding vectors about W(6) is presumed to be approximately dodecahedral, with one vector towards each of the five exopolyhedral $(PMe_2Ph)_3H_2$ ligands, one towards each of the two W–H–B bridging hydrides, and one directed towards a tangential bond with B(2)

Table 1. Selected interatomic distances (pm) for [6,6,6,6,6-$(PMe_2Ph)_3H_2$-6-WB_9H_{13}] (**1**) with estimated standard deviations (e.s.d.s) in parentheses

(*i*) From the tungsten atom			
W(6)–P(1)	245.8(5)	W(6)–B(2)	243.2(14)
W(6)–P(2)	249.4(5)	W(6)–B(5)	241.8(14)
W(6)–P(3)	242.2(5)	W(6)–B(7)	247.2(16)
(*ii*) Boron–boron			
B(1)–B(2)	174.6(19)	B(2)–B(3)	175.9(20)
B(1)–B(3)	175.1(21)		
B(1)–B(5)	173.8(19)	B(3)–B(7)	174.2(18)
B(1)–B(4)	177.4(21)	B(3)–B(4)	178.3(20)
B(1)–B(10)	171.4(20)	B(3)–B(8)	173.5(20)
B(2)–B(5)	177.9(20)	B(2)–B(7)	182.5(21)
B(4)–B(9)	173.6(19)		
B(4)–B(8)	174.2(20)	B(4)–B(10)	177.7(21)
B(5)–B(10)	205.3(22)	B(7)–B(8)	197.6(21)
B(9)–B(10)	179.3(21)	B(8)–B(9)	178.5(20)
(*iii*) Boron–hydrogen			
B(1)–H(1)	112(6)	B(3)–H(3)	111(6)
B(5)–H(5)	99(7)	B(7)–H(7)	105(6)
B(10)–H(10)	111(6)	B(8)–H(8)	98(6)
B(2)–H(2)	103(7)		
B(9)–H(9)	116(6)		
B(4)–H(4)	105(6)		
B(8)–H(8,9)	110(6)	B(10)–H(9,10)	128(6)
B(9)–H(8,9)	126(6)	B(9)–H(9,10)	111(7)

(neutral) metal centre $WH_2(PMe_2Ph)_3$ can be thought of as contributing three orbitals and two electrons to the cluster bonding scheme, just like BH. Compound (**1**) can therefore be regarded as an 18-electron d^2 tungsten(IV) complex, with five two-electron bonds to the five *exo*-polyhedral ligands $H_2(PMe_2Ph)_3$ and three two-electron bonds to the cluster. The overall stereochemistry of the located atoms about tungsten

Table 2. Selected angles (°) between interatomic vectors for [6,6,6,6,6-$(PMe_2Ph)_3H_2$-6-WB_9H_{13}] (**1**) with e.s.d.s in parentheses

(*i*) At the tungsten atom			
P(1)–W(6)–P(2)	90.3(2)		
P(1)–W(6)–P(3)	128.5(2)	P(2)–W(6)–P(3)	101.0(2)
P(1)–W(6)–B(5)	82.9(4)	P(2)–W(6)–B(7)	77.2(4)
P(1)–W(6)–B(2)	91.3(4)	P(2)–W(6)–B(2)	92.5(4)
P(1)–W(6)–B(7)	131.4(3)	P(2)–W(6)–B(5)	134.5(3)
P(3)–W(6)–B(2)	137.3(3)		
P(3)–W(6)–B(5)	118.4(4)	P(3)–W(6)–B(7)	100.1(4)
B(5)–W(6)–B(2)	43.0(4)	B(7)–W(6)–B(2)	43.7(4)
B(5)–W(6)–B(7)	74.3(5)		
(*ii*) Tungsten–boron–boron			
W(6)–B(5)–B(1)	122.4(9)	W(6)–B(7)–B(3)	121.3(10)
W(6)–B(5)–B(2)	68.9(6)	W(6)–B(7)–B(2)	67.0(7)
W(6)–B(5)–B(10)	125.0(9)	W(6)–B(7)–B(8)	124.7(8)
W(6)–B(2)–B(1)	121.3(9)	W(6)–B(2)–B(3)	122.6(9)
W(6)–B(2)–B(5)	68.1(6)	W(6)–B(2)–B(7)	69.3(7)
(*iii*) Others			
B(7)–B(8)–B(9)	119.2(10)	B(5)–B(10)–B(9)	117.9(10)
B(8)–B(9)–B(10)	103.2(10)		
B(8)–H(8,9)–B(9)	98(4)	B(9)–H(9,10)–B(10)	94(4)

suggests an approximate dodecahedral distribution for the eight bonding vectors.

The reaction of *mer*-$[OsCl_3(PMe_2Ph)_3]$ with $[NBu_4][B_9H_{14}]$ in boiling ethanol rapidly afforded the orange osmaborane [6,6,6-$(PMe_2Ph)_3$-*nido*-6-OsB_9H_{13}] (**3**) in 32% yield and the analogous red ruthenaborane [6,6,6-$(PMe_2Ph)_3$-*nido*-6-RuB_9H_{13}] (**4**) was obtained in similar yield from the corresponding ruthenium complex *mer*-$[RuCl_3(PMe_2Ph)_3]$. *X*-Ray diffraction analysis revealed the molecular structure of compound (**3**) as shown in Figure 2. In this case all atoms were located and the structural similarity to *nido*-$B_{10}H_{14}$ is again apparent. Selected interatomic distances and angles are in Tables 3 and 4. Again the retention of the diagnostically long distances B(5)–B(10) and B(7)–B(8) is noteworthy, and again the (neutral) metal centre $Os(PMe_2Ph)_3$ can be thought of as contributing three orbitals and two electrons to the cluster bonding scheme, just like BH in $B_{10}H_{14}$. Compound (**3**) can therefore be regarded as an octahedral 18-electron d^6 osmium(II) complex, with three two-electron bonds to the three exopolyhedral ligands $(PMe_2Ph)_3$, and three two-electron bonds to the cluster. These last three bonding vectors will be directed principally towards H(5,6), H(6,7), and a bond with B(2) which will have its maximum electron density tangential to the cluster, approximately *trans* to the axial phosphorus atom P(3) (Figure 2).

Structural data for the precisely analogous dimethylphenylphosphine *nido*-iridadecaborane are not available but the crystal and molecular structure of the closely related triphenylphosphine compound [6,6,6-$(PPh_3)_2$H-*nido*-6-IrB_9H_{13}] (**5**) has been determined.[8] This permits a detailed comparison of the structures of the *nido*-6-metalladecaboranes for the four adjacent third-row transition metals tungsten, rhenium, osmium, and iridium. Table 5 summarizes the metal–boron and metal–phosphorus distances in the four compounds and the trends are readily apparent from Figure 3: the M–B(2) distance decreases by *ca.* 5.4 ± 1.3 pm for each unit increase in atomic number of the metal atom and the mean decrease in the M–B(5,7) distance is similar (5.3 pm) although less regular. With the M–P distances there is some evidence that the decreases progressively diminish with successive unit increase in atomic number. Thus for M–P(axial) the successive decreases in

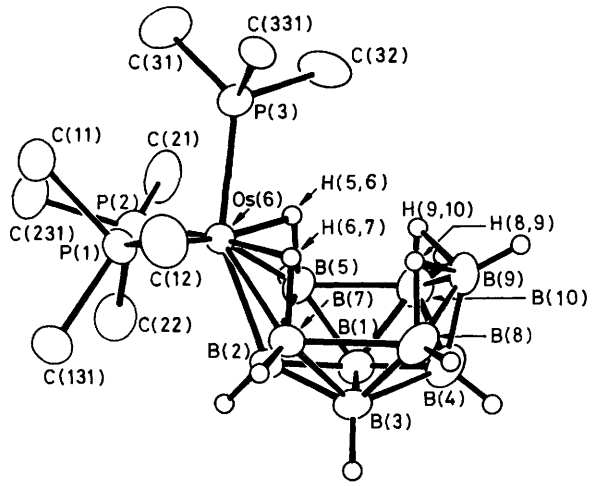

Figure 2. Molecular structure of $[(PMe_2Ph)_3OsB_9H_{13}]$ (**3**) with selected P-organyl group atoms omitted for clarity

Table 3. Selected interatomic distances (pm) for $[6,6,6\text{-}(PMe_2Ph)_3\text{-}6\text{-}OsB_9H_{13}]$ (**3**) with e.s.d.s in parentheses

(*i*) From the osmium atom			
Os(6)–P(1)	234.4(3)	Os(6)–B(2)	233.7(7)
Os(6)–P(2)	234.1(3)	Os(6)–B(5)	234.4(7)
Os(6)–P(3)	231.9(3)	Os(6)–B(7)	224.3(7)
Os(6)–H(5,6)	166(3)	Os(6)–H(6,7)	167(4)
(*ii*) Boron–boron			
B(1)–B(2)	176.3(9)	B(2)–B(3)	177.6(10)
B(1)–B(3)	177.1(10)		
B(1)–B(5)	174.3(10)	B(3)–B(7)	177.3(9)
B(1)–B(4)	179.4(10)	B(3)–B(4)	179.7(10)
B(1)–B(10)	174.3(10)	B(3)–B(8)	172.9(10)
B(2)–B(5)	179.5(9)	B(2)–B(7)	178.8(10)
B(4)–B(9)	168.0(11)		
B(4)–B(8)	174.5(10)	B(4)–B(10)	176.6(11)
B(5)–B(10)	201.6(10)	B(7)–B(8)	208.3(11)
B(9)–B(10)	177.7(11)	B(8)–B(9)	175.9(11)
(*iii*) Boron–hydrogen			
B(1)–H(1)	115(4)	B(3)–H(3)	112(5)
B(5)–H(5)	120(4)	B(7)–H(7)	111(4)
B(10)–H(10)	114(5)	B(8)–H(8)	108(5)
B(2)–H(2)	109(4)		
B(9)–H(9)	103(5)		
B(4)–H(4)	102(5)		
B(5)–H(5,6)	140(4)	B(7)–H(6,7)	135(4)
B(10)–H(9,10)	137(5)	B(8)–H(8,9)	130(5)
B(9)–H(9,10)	131(5)	B(9)–H(8,9)	132(5)

the sequence W ⟶ Re ⟶ Os ⟶ Ir are 6.9, 3.4, and 1.4 pm respectively whereas for the mean M–P(equatorial) distances the successive decreases are 7.4, 6.0, and 4.0 pm respectively.

N.M.R. Properties.—The ^{11}B and ^{1}H n.m.r. chemical shifts for the series of compounds are summarized with assignments in Table 6.

The general pattern of ^{11}B shielding behaviour (Figure 4) is very similar to that of *nido*-$B_{10}H_{14}$ (also included in Figure 4 and Table 6 for comparison). The B(1)(3), B(4), and B(8)(10) sites distant from the metal centre are little affected by the presence of the metal centre, the changes being only *ca.* 5

Table 4. Selected angles (°) between interatomic vectors for $[6,6,6\text{-}(PMe_2Ph)_3\text{-}6\text{-}OsB_9H_{13}]$ (**3**) with e.s.d.s in parentheses

(*i*) At the osmium atom			
P(1)–Os(6)–P(2)	97.4		
P(1)–Os(6)–P(3)	92.0	P(2)–Os(6)–P(3)	95.6
P(1)–Os(6)–B(5)	155.9(1)	P(2)–Os(6)–B(7)	136.5(1)
P(1)–Os(6)–B(2)	111.3(2)	P(2)–Os(6)–B(2)	95.0(2)
P(1)–Os(6)–B(7)	84.3(2)	P(2)–Os(6)–B(5)	82.6(2)
P(3)–Os(6)–B(2)	152.9(1)		
P(3)–Os(6)–B(5)	112.1(2)	P(3)–Os(6)–B(7)	127.8(2)
P(1)–Os(6)–H(5,6)	166.5(11)	P(2)–Os(6)–B(6,7)	173.3(12)
P(1)–Os(6)–H(6,7)	83.5(13)	P(2)–Os(6)–H(5,6)	90.8(12)
P(3)–Os(6)–H(5,6)	76.4(12)	P(3)–Os(6)–H(6,7)	90.9(13)
B(5)–Os(6)–B(2)	45.1(2)	B(7)–Os(6)–B(2)	45.9(2)
B(5)–Os(6)–B(7)	79.5(3)		
(*ii*) Osmium–boron–boron			
Os(6)–B(5)–B(1)	119.3(4)	Os(6)–B(7)–B(3)	122.3(4)
Os(6)–B(5)–B(2)	67.3(3)	Os(6)–B(7)–B(2)	69.9(3)
Os(6)–B(5)–B(10)	118.8(4)	Os(6)–B(7)–B(8)	121.7(4)
Os(6)–B(2)–B(1)	118.7(4)	Os(6)–B(2)–B(3)	117.2(4)
Os(6)–B(2)–B(5)	67.6(8)	Os(6)–B(2)–B(7)	64.2(3)
(*iii*) Others			
Os(6)–H(5,6)–B(5)	100(3)	Os(6)–H(6,7)–B(7)	95(2)
B(9)–H(9,10)–B(10)	83(3)	B(9)–H(8,9)–B(8)	84(3)
B(5)–B(10)–B(9)	118.7(4)	B(7)–B(8)–B(9)	115.6(5)
B(10)–B(9)–B(8)	105.9(5)		

Table 5. Comparison of metal–ligand distances (pm) in compounds (**1**), (**2**), (**3**), and (**5**)

	M			
	W (**1**)	Re (**2**)	Os (**3**)	Ir (**5**)
M–B(2)	243.2(14)	237.8(5)	233.7(7)	226.9(8)
M–B(5)	241.8(14)	236.6(5)	234.4(7)	228.9(9)
M–B(7)	247.2(16)	238.6(5)	224.3(7)	228.1(11)
M–P(axial)	242.2(5)	235.3(3)	231.9(3)	230.5(2)
M–P(equatorial)	245.8(5) 249.4(5)	240.4(3) 240.0(3)	234.1(3) 234.4(3)	230.3(2)

p.p.m. at most. This sort of variation, for example, is comparable to changes induced at these sites by *trans* effects of different *ligands* on the *same* metal centre,[4,8] and it is at first sight surprising that the variation in the metal across the W ⟶ Re ⟶ Os ⟶ Ir sequence results in so small a change. Interestingly, the remaining position distant from the metal, at B(9), gives greater deviations, but only for two of the metals (W and Os) and then only 7 p.p.m. or so. The sites adjacent to the metal centre are also little affected, generally by no more than the distant ones, the exceptions being the B(2) position for the wolfraborane (a deshielding of *ca.* 14 p.p.m.) and the B(5)(7) positions for the rhena- and osma-boranes (*ca.* 10—12 p.p.m.). These may reflect different principal axes of electronic circulation at the metal centre which may be imposed by the *exo*-polyhedral phosphine and hydrogen ligand dispositions about the metal. In all these *nido*-6-metalladecaboranes a general lowering of nuclear shielding of the B(2) and B(5)(7) boron nuclei adjacent to the metal centres may be expected as the metal-to-boron bonding electrons would be expected to have easier access to the lower excited states that would presumably be associated with the transition-metal centre. Even

Table 6. Boron-11 and proton n.m.r. data for $[(PMe_2Ph)_3H_2WB_9H_{13}]$ (**1**), $[(PMe_2Ph)_3HReB_9H_{13}]$ (**2**), $[(PMe_2Ph)_3OsB_9H_{13}]$ (**3**), and $[(PMe_2Ph)_3RuB_9H_{13}]$ (**4**), in $CDCl_3$ solution at +21 °C compared with similar data for $[(PMe_3)_2HIrB_9H_{13}]$ (**6**) and *nido*-$B_{10}H_{14}$

	W (1)[a,b]		Re (2)[c]		Os (3)[a,d]		Ru (4)[a,e]		Ir (6)[f]		$B_{10}H_{14}$[g]	
Assignment	δ(^{11}B)	δ(^{1}H)	δ(^{11}B)	δ(^{1}H)	δ(^{11}B)	δ(^{1}H)	δ(^{11}B)	δ(^{1}H)	δ(^{11}B)	δ(^{1}H)	δ(^{11}B)	δ(^{1}H)
5,7	+7.2	+4.40	+12.2	+5.11	+11.43	+5.18	+12.91	+4.19	+8.1, +3.4	+5.41, +3.27	−0.4	+3.13
1,3	+12.3	+4.05	+10.2	+4.51	+8.81	+4.29	+10.25	+3.44	+10.5, +9.2	+4.56, +4.32	+11.7	+3.68
9	+2.5	+2.70	+5.5	+2.60	+3.0	+3.13	+2.38	+2.93	+10.5	+4.89	+9.8	+3.85
8,10	+3.0	+2.87	−1.5	+2.60	−1.6	+2.76	−1.39	+2.73	−0.2, −2.2	+3.04, +2.94	−0.4	+3.13
2	−23.1	−0.37	−29.8	−0.30	−29.23	−0.17	−23.2	−0.06	−31.5	−0.40	−36.4	+0.55
4	−33.0	+1.51	−29.0	+2.06	−31.27	+1.81	−30.7	+1.05	−31.5	+2.17	−36.4	+0.65
Bridge BHB	—	−3.61	—	−4.20	—	−3.93	—	−3.47	—	−3.69	—	−2.14
Bridge MHB	—	−8.59	—	−10.74	—	−11.27	—	−11.14	—	−7.78, −10.60	—	—
M(6)–H	—	−2.22[h]	—	−5.54[h]	—	—	—	—	—	−13.03[h]	—	—

[a] This work. [b] δ(^{31}P) −6.1 p.p.m., $^1J(^{183}W-^{31}P)$ *ca.* 227 Hz. [c] Data from ref. 7; δ(^{31}P) −15.9 p.p.m. [d] δ(^{31}P) −26.9 (2 P) and −29.3 (1 P) p.p.m., $^2J(^{31}P-^{31}P)$ *ca.* 22 Hz. [e] δ(^{31}P) +13.8 (2 P) and +14.5 (1 P) p.p.m., $^2J(^{31}P-^{31}P)$ *ca.* 25 Hz ($CDCl_3$ solution at −50 °C). [f] Data from ref. 8; δ(^{31}P) +19.2 (1 P) and +14.6 (1 P) p.p.m., $^2J(^{31}P-^{31}P)$ *ca.* 21 Hz ($CDCl_3$ solution at −47 °C). [g] Data from refs. 32 and 33. [h] Multiplet due to couplings $^2J(^{31}P-^1H)$ and [for compound (**6**)] $^2J(^1H-^1H)$.

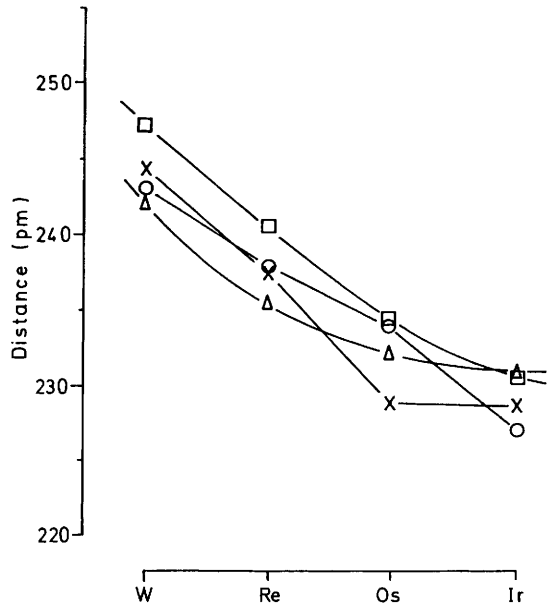

Figure 3. Interatomic distances from the metal atom in the four complexes, $[(PMe_2Ph)_3H_2WB_9H_{13}]$ (**1**), $[(PMe_2Ph)_3HReB_9H_{13}]$ (**2**), $[(PMe_2Ph)_3OsB_9H_{13}]$ (**3**), and $[(PPh_3)_2HIrB_9H_{13}]$ (**5**), to B(2) (○), to B(5,7) (×), to P(axial) (△), and to P(equatorial) (□)

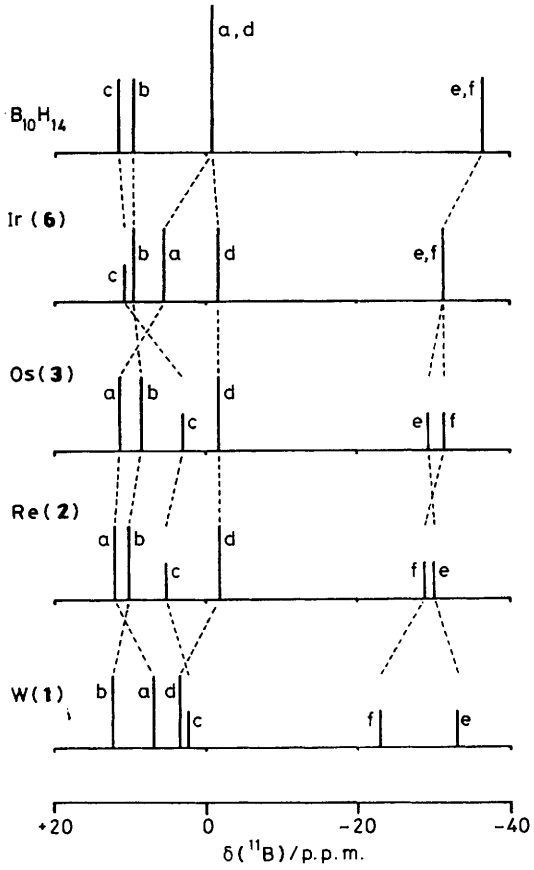

Figure 4. Stick diagram of the ^{11}B n.m.r. positions for $[(PMe_2Ph)_3H_2WB_9H_{13}]$ (**1**), $[(PMe_2Ph)_3HReB_9H_{13}]$ (**2**), $[(PMe_2Ph)_3OsB_9H_{13}]$ (**3**), $[(PMe_3)_2HIrB_9H_{13}]$ (**6**), and $B_{10}H_{14}$. Mean resonance positions have been plotted for the asymmetric species $[(PMe_3)_2HIrB_9H_{13}]$ (**6**), and it should also be noted that the ^{11}B(2) and ^{11}B(4) resonances are accidentally coincident for this compound. Assignments are ^{11}B(5,7) a, ^{11}B(1,3) b, ^{11}B(9) c, ^{11}B(8,10) d, ^{11}B(2) e, and ^{11}B(4) f. Resonances e and f are assigned on the basis of ^{1}H shielding behaviour (Figure 5 and refs. 7 and 14)

so, these changes are small, particularly for the osma- and iridaboranes so that it is reasonable to conclude that the overall gross properties of the ground and lower-excited states for the valence electrons in these *nido*-6-metalladecaborane clusters are little perturbed from that in *nido*-$B_{10}H_{14}$ itself. Indeed, the changes induced in the *nido*-decaboranyl shieldings on replacement of a BH vertex by these very disparate third-row transition metal centres are, if anything, somewhat less than those induced in *nido*-decaboranyl clusters by simple substitution of an *exo*-terminal hydrogen atom by a halogen, for example.[10,11] This serves to emphasize the compatability of these types of metal centre with the polyhedral boron clusters.

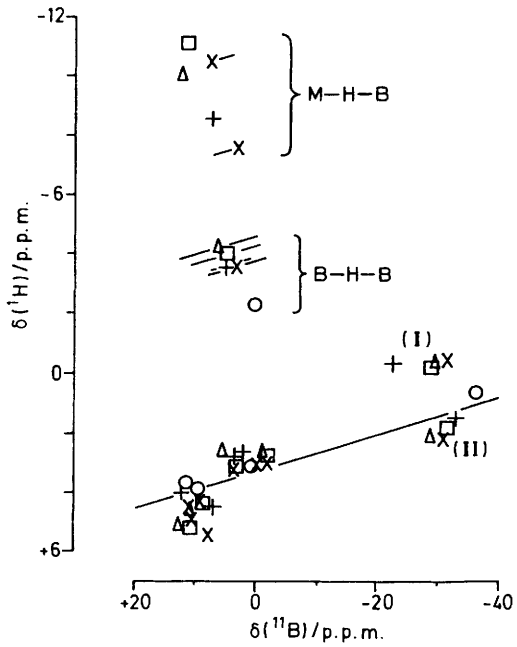

Figure 5. Proton–boron-11 shielding correlation plot for the metallaboranes $[(PMe_2Ph)_3H_2WB_9H_{13}]$ (**1**) (+), $[(PMe_2Ph)_3HReB_9H_{13}]$ (**2**) (△), $[(PMe_2Ph)_3OsB_9H_{13}]$ (**3**) (□), and $[(PMe_3)_2HIrB_9H_{13}]$ (**6**) (×). The line drawn has slope δ(¹¹B):δ(¹H) of 16:1 (*cf.* refs. 4, 7, and 16). The close groupings of data points indicate the parallels in electronic structure across the sequence. The (2, 4) resonance data associated with the higher proton shielding [points (**I**)] are ascribed to the 2-positions by analogy with the 6-rhenadecaboranes (ref. 7)

In accord with broad metallaborane shielding correlations noted elsewhere,[4,5,7,11–17] the proton shielding in the cluster *exo*-terminal hydrogen atoms broadly parallels that of the nuclear shielding of the boron atoms to which they are directly bound (Figure 5), with the $^1H(2)$ resonances [points (**I**)] being relatively to somewhat higher field than the $^1H(4)$ resonances [points (**II**)], again as previously noted in *nido*-6-metalladecaboranes.[4,7] The metal–terminal proton shielding is progressively higher in the sequence W ⟶ Re ⟶ Os ⟶ Ir, as is often generally observed. For the wolfraborane (**1**) it is of interest that only one W–terminal resonance is observed in the proton spectrum, and only one resonance in the ^{31}P spectrum, which suggests that this compound is also fluxional in a similar manner to the previously reported[7] rhenaborane (**2**).

The stability of the compounds reported here augers well for an extensive polyhedral metallaborane cluster chemistry of these elements; this is already apparent for iridium,[6,8,18] whereas other reports of osmaborane[19–22] and rhenaborane[7,23,24] chemistry remain relatively limited so far. The tungsten compound reported here is the first structurally characterised wolfraborane; the only previously reported wolfraboranes are the species $[(\eta^5\text{-}C_5H_5)(CO)_2WB_3H_8]$, $[(CO)_4WB_3H_8]^-$, and $[(CO)_4WB_{10}H_{12}]^{2-}$.[25–28]

Experimental

General.—The starting metal complexes $[WH_6(PMe_2Ph)_3]$, $[ReH_5(PMe_2Ph)_3]$, $[OsCl_3(PMe_2Ph)_3]$, and $[RuCl_3(PMe_2Ph)_3]$ were prepared by standard methods.[29–31] $B_{10}H_{14}$ was sublimed (0.1 mmHg/80 °C) before use and $[NR_4][B_9H_{14}]$ (R = Et or Bu) was prepared from it by published methods.[14] Absolute ethanol was used as supplied and CH_2Cl_2 was refluxed over and distilled from CaH_2 before use. Nitrogen gas was dried by passage through concentrated H_2SO_4 and then through KOH pellets.

N.M.R. Studies.—100-MHz ^1H, $^1H\text{-}\{^{11}B\}$ and $^1H\text{-}\{^{31}P\}$, 32-MHz ^{11}B and $^{11}B\text{-}\{^1H\}$, and 40-MHz $^{31}P\text{-}\{^1H\}$ n.m.r. experiments were performed on a JEOL FX-100 pulse [Fourier-transform (F.t.)] spectrometer. 128-MHz ^{11}B and $^{11}B\text{-}\{^1H\}$ experiments were performed on a Bruker WH-400 pulse (F.t.) spectrometer at the S.E.R.C. service centre at Sheffield University. 115.5-MHz ^{11}B and 360-MHz $^1H\text{-}\{^{11}B\}$ n.m.r. experiments were performed at Edinburgh University S.E.R.C. service centre on a Bruker WH-360 pulse (F.t.) spectrometer. General conditions for $^1H\text{-}\{^{11}B(selective)\}$ n.m.r. spectroscopy have been discussed elsewhere.[8,12–14,32,33] Other spectroscopy was straightforward. Solutions and conditions are specified in Table 6. Chemical shifts (δ) are given in p.p.m. to high frequency (low field) of $SiMe_4$ for ^1H, of 85% H_3PO_4 [Ξ 40 480 730 Hz] for ^{31}P, and of $BF_3(OEt_2)$ in $CDCl_3$ [Ξ 32 083 971 Hz][11] for ^{11}B.

Preparation of $[(PMe_2Ph)_3H_2WB_9H_{13}]$ (**1**).—To a deoxygenated solution of $[WH_6(PMe_2Ph)_3]$ (600 mg, 1.0 mmol) in CH_2Cl_2 (30 cm^3) was added *via* a 'tipper tube' solid $[NEt_4][B_9H_{14}]$ (500 mg, 2.0 mmol). The reaction mixture was stirred for 2 d at room temperature under an atmosphere of dry nitrogen. Subsequent manipulations were carried out in air. The solvent was evaporated under reduced pressure (30 °C/water pump), and the residual small volume (*ca.* 3 cm^3) applied to a series of preparative t.l.c. plates (20 × 20 × 0.1 cm; silica, Kieselgel GF 254) which were developed using CH_2Cl_2 as eluant. The blue-green band (R_f 0.9) was removed from the preparative t.l.c. plates and separated from the silica by washing with dry CH_2Cl_2 (25 cm^3). Further chromatography on this component using light petroleum (b.p. 60—80 °C)–CH_2Cl_2 (1:1) as the solvent system gave this component pure (R_f 0.5). The product, a microcrystalline halcyon-blue solid, $[(PMe_2Ph)_3H_2WB_9H_{13}]$ (**1**), was obtained in 21% yield (130 mg). A crystal of this compound suitable for a single-crystal *X*-ray diffraction analysis was obtained by diffusion of cyclohexane at room temperature into a solution of the compound in 1,2-$C_2H_4Cl_2$. The n.m.r. properties of this compound can be found in Table 6.

Preparation of $[(PMe_2Ph)_3HReB_9H_{13}]$ (**2**).—A procedure identical to that outlined above for compound (**1**) was used with $[ReH_5(PMe_2Ph)_3]$ as the starting metal complex. This gave the previously reported[7] compound $[(PMe_2Ph)_3HReB_9H_{13}]$ in a much improved yield (*ca.* 65%) as a purple microcrystalline solid. This product was characterised by comparison of its n.m.r. properties with those of an authentic sample.

Preparation of $[(PMe_2Ph)_3OsB_9H_{13}]$ (**3**).—To a deoxygenated solution of $[OsCl_3(PMe_2Ph)_3]$ (140 mg, 0.2 mmol) in absolute ethanol (50 cm^3) was added an excess (10:1) of solid $[NBu_4][B_9H_{14}]$ (650 mg, 2.0 mmol). The reaction mixture was refluxed for 20 min under an atmosphere of dry nitrogen and subsequent manipulations were carried out in air. The solvent was removed under reduced pressure (30 °C/water pump) and the residue dissolved in dry CH_2Cl_2 (*ca.* 3 cm^3) and applied to a series of preparative silica t.l.c. plates which were developed using CH_2Cl_2 as eluant. The orange band (R_f 0.8) was rechromatographed until pure and gave, upon crystallisation from CH_2Cl_2–cyclohexane, an orange microcrystalline solid $[(PMe_2Ph)_3OsB_9H_{13}]$ (**3**) in 32% yield (37 mg). A single crystal suitable for an *X*-ray diffraction analysis was grown by diffusion of solvents (CH_2Cl_2–cyclohexane) at 4 °C. The n.m.r. parameters of this compound can be found in Table 6.

Table 7. Atomic co-ordinates ($\times 10^4$) for $[6,6,6,6,6\text{-}(PMe_2Ph)_3H_2\text{-}6\text{-}WB_9H_{13}]$ (**1**) with e.s.d.s in parentheses

Atom	*x*	*y*	*z*
W(6)	4 774(0.2)	2 526(0.4)	7 464(0.2)
P(1)	4 564(2)	2 445(3)	6 210(1)
P(2)	6 240(2)	1 635(2)	7 417(2)
P(3)	4 197(2)	1 120(3)	8 294(2)
C(11)	5 415(8)	3 047(11)	5 719(7)
C(12)	4 457(8)	843(10)	5 836(7)
C(131)	3 618(3)	3 207(5)	5 772(3)
C(132)	2 829(3)	2 601(5)	5 785(3)
C(133)	2 107(3)	3 135(5)	5 439(3)
C(134)	2 174(3)	4 274(5)	5 081(3)
C(135)	2 963(3)	4 880(5)	5 063(3)
C(136)	3 685(3)	4 346(5)	5 413(3)
C(21)	6 804(7)	1 013(10)	8 203(6)
C(22)	7 053(8)	2 737(10)	7 180(6)
C(231)	6 368(4)	262(5)	6 850(3)
C(232)	5 931(4)	−864(5)	6 970(3)
C(233)	6 026(4)	−1 923(5)	6 552(3)
C(234)	6 558(4)	−1 855(5)	6 014(3)
C(235)	6 994(4)	−729(5)	5 895(3)
C(236)	6 899(4)	330(5)	6 313(3)
C(31)	3 581(7)	−230(10)	7 960(6)
C(32)	4 905(8)	356(11)	8 948(6)
C(331)	3 434(4)	1 937(5)	8 821(3)
C(332)	3 653(4)	2 287(5)	9 497(3)
C(333)	3 062(4)	2 920(5)	9 872(3)
C(334)	2 252(4)	3 201(5)	9 570(3)
C(335)	2 033(4)	2 851(5)	8 894(3)
C(336)	2 624(4)	2 218(5)	8 519(3)
B(1)	4 646(9)	5 988(12)	7 644(8)
B(2)	5 285(9)	4 711(12)	7 428(7)
B(3)	5 558(9)	5 606(12)	8 171(8)
B(4)	4 679(9)	6 368(12)	8 527(7)
B(5)	4 154(8)	4 623(11)	7 301(7)
B(7)	5 647(9)	3 954(12)	8 236(8)
B(8)	5 191(9)	5 071(12)	8 933(8)
B(9)	4 064(9)	5 277(12)	8 938(7)
B(10)	3 751(9)	5 736(11)	8 075(7)

Table 8. Atomic co-ordinates ($\times 10^4$) for $[6,6,6\text{-}(PMe_2Ph)_3\text{-}6\text{-}OsB_9H_{13}]$ (**3**) with e.s.d.s in parentheses

Atom	*x*	*y*	*z*
Os(6)	1 181(0.2)	2 395(0.1)	9 816(0.1)
P(1)	3 239(1)	3 037(1)	9 889(1)
P(2)	−286(1)	3 196(1)	9 166(1)
P(3)	1 783(1)	1 864(1)	8 653(1)
C(11)	3 859(5)	3 379(3)	8 959(3)
C(12)	4 821(5)	2 575(3)	10 245(4)
C(131)	3 344(3)	3 773(1)	10 566(2)
C(132)	2 224(3)	3 926(1)	11 024(2)
C(133)	2 295(3)	4 483(1)	11 531(2)
C(134)	3 487(3)	4 888(1)	11 580(2)
C(135)	4 608(3)	4 735(1)	11 121(2)
C(136)	4 536(3)	4 178(1)	10 615(2)
C(21)	−1 704(5)	2 887(3)	8 477(3)
C(22)	−1 328(5)	3 686(3)	9 837(4)
C(231)	421(4)	3 890(2)	8 582(2)
C(232)	995(4)	4 449(2)	8 987(2)
C(233)	1 526(4)	4 981(2)	8 557(2)
C(234)	1 482(4)	4 953(2)	7 722(2)
C(235)	909(4)	4 394(2)	7 317(2)
C(236)	378(4)	3 863(2)	7 747(2)
C(31)	1 577(7)	2 231(3)	7 649(3)
C(32)	732(6)	1 108(3)	8 462(4)
C(331)	3 546(3)	1 506(2)	8 661(2)
C(332)	3 952(3)	1 029(2)	9 244(2)
C(333)	5 295(3)	756(2)	9 271(2)
C(334)	6 233(3)	959(2)	8 717(2)
C(335)	5 827(3)	1 436(2)	8 135(2)
C(336)	4 483(3)	1 709(2)	8 107(2)
B(1)	−1 031(6)	1 768(3)	11 253(4)
B(2)	89(6)	2 433(3)	11 022(3)
B(3)	639(6)	1 838(3)	11 771(3)
B(4)	−158(6)	1 025(3)	11 635(4)
B(5)	−938(5)	1 993(3)	10 250(3)
B(7)	1 845(6)	2 122(3)	11 087(3)
B(8)	1 620(6)	1 149(3)	11 521(4)
B(9)	578(7)	608(3)	10 898(4)
B(10)	−1 017(7)	1 044(3)	10 666(4)

Preparation of $[(PMe_2Ph)_3RuB_9H_{13}]$ (**4**).—In an analogous manner to (**3**), compound (**4**) was prepared in *ca.* 35% yield (42 mg) as a red microcrystalline solid from the reaction of $[RuCl_3(PMe_2Ph)_3]$ (120 mg, 0.2 mmol) and $[NBu_4][B_9H_{14}]$ (650 mg, 2.0 mmol) in refluxing ethanol (50 cm^3). This compound has an R_f value of 0.8 in CH_2Cl_2 and was characterised by multielement F.t. n.m.r. spectroscopy (see Table 6 and the Results and Discussion section).

X-*Ray Studies*.—All crystallographic measurements were made using a Syntex $P2_1$ diffractometer operating in the ω–2θ scan mode using graphite-monochromated Mo-K_α radiation (λ = 71.069 pm) and following a procedure described in detail elsewhere.[34] Both sets of data were corrected for absorption empirically.[35] Structure solution and refinement for both compounds was *via* standard heavy-atom procedures and full-matrix least squares using the SHELX program system.[36] For $[(PMe_2Ph)_3OsB_9H_{13}]$ (**3**) all non-hydrogen atoms were refined with anisotropic thermal parameters while for $[(PMe_2Ph)_3H_2WB_9H_{13}]$ (**1**) only the W and P atoms were assigned anisotropic thermal parameters; all other non-hydrogen atoms in (**1**) were refined with isotropic thermal parameters. In both cases all phenyl and methyl hydrogens were included in calculated positions (C–H = 1.08 pm) using the AFIX routines in the SHELX program and were assigned an overall isotropic thermal parameter for each group. All other hydrogen atoms were located experimentally (apart from those attached both terminally and bridging to the W atom, which were not located) and were freely refined with individual isotropic thermal parameters. For both compounds the weighting scheme $w = [\sigma^2(F_o) + g(F_o)^2]^{-1}$ was used in which the parameter g was included in refinement to give a flat analysis of variance with increasing sinθ and $[F/F_{max.}]^{\frac{1}{2}}$.

Crystal data for $[(PMe_2Ph)_3H_2WB_9H_{13}]$ (**1**). $C_{24}H_{48}B_9P_3W$, M = 710.81, monoclinic, a = 1 571.7(5), b = 1 049.1(5), c = 1 961.5(8) pm, β = 94.30(3)°, U = 3.225 nm^3, space group $P2_1/n$ (= $P2_1/c$, no. 14), Z = 4, D_c = 1.46 g cm^{-3}, μ(Mo-K_α) = 35.65 cm^{-1}, F(000) = 1 404, T = 290 K.

Data collection. Scans running from 1° below $K_{\alpha 1}$ to 1° above $K_{\alpha 2}$, scan speeds 2.0—29.3° min^{-1}, 4.0 < 2θ < 45.0°. 4 517 Unique data, 3 139 observed [$I > 2\sigma(I)$].

Structure refinement. Number of parameters = 204, weighting factor g = 0.0002, R = 0.0512, R' = 0.0526.

Crystal data for $[(PMe_2Ph)_3OsB_9H_{13}]$ (**3**). $C_{24}H_{46}B_9OsP_3$, M = 715.14, monoclinic, a = 957.8(1), b = 1 990.0(4), c = 1 671.4(3) pm, β = 94.01(1)°, U = 3.178 nm^3, space group $P2_1/c$, Z = 4, D_c = 1.49 g cm^{-3}, μ(Mo-K_α) = 39.92 cm^{-1}, F(000) = 1 424, T = 290 K.

Data collection. Parameters as above. 4 430 Unique data, 3 948 observed [$I > 2\sigma(I)$].

Structure refinement. Number of parameters = 377, weighting factor g = 0.0001, R = 0.0240, R' = 0.0232.

Lists of final atomic co-ordinates for compounds (**1**) and (**3**) are in Tables 7 and 8 respectively.

Acknowledgements

We thank the S.E.R.C. for support.

References

1 R. N. Grimes (ed.), 'Metal Interactions with Boron Clusters,' Plenum Press, New York, 1982.
2 N. N. Greenwood, *Pure Appl. Chem.*, 1983, **55**, 1415; *Chem. Soc. Rev.*, 1984, **13**, 353.
3 J. D. Kennedy, *Prog. Inorg. Chem.*, 1984, **32**, 519; 1986, **34**, in the press.
4 N. N. Greenwood, J. D. Kennedy, M. Thornton-Pett, and J. D. Woollins, *J. Chem. Soc., Dalton Trans.*, 1985, 2397.
5 J. E. Crook, M. Elrington, N. N. Greenwood, J. D. Kennedy, M. Thornton-Pett, and J. D. Woollins, *J. Chem. Soc., Dalton Trans.*, 1985, 2407.
6 J. Bould, Ph.D. Thesis, University of Leeds, 1983.
7 M. A. Beckett, N. N. Greenwood, J. D. Kennedy, and M. Thornton-Pett, *J. Chem. Soc., Dalton Trans.*, 1985, 1119.
8 S. K. Boocock, J. Bould, N. N. Greenwood, J. D. Kennedy, and W. S. McDonald, *J. Chem. Soc., Dalton Trans.*, 1982, 713.
9 A. Tippe and W. C. Hamilton, *Inorg. Chem.*, 1969, **8**, 1464.
10 R. Ahmad, Ph.D. Thesis, University of Leeds, 1982.
11 J. D. Kennedy, in 'Multinuclear N.M.R.,' ed. J. Mason, Plenum Press, London and New York, 1986, ch. 8, in the press.
12 J. D. Kennedy and B. Wrackmeyer, *J. Magn. Reson.*, 1980, **38**, 529.
13 J. D. Kennedy and N. N. Greenwood, *Inorg. Chim. Acta*, 1980, **38**, 93.
14 S. K. Boocock, N. N. Greenwood, M. J. Hails, J. D. Kennedy, and W. S. McDonald, *J. Chem. Soc., Dalton Trans.*, 1981, 1415.
15 J. E. Crook, N. N. Greenwood, J. D. Kennedy, and W. S. McDonald, *J. Chem. Soc., Dalton Trans.*, 1984, 2487.
16 N. N. Greenwood, M. J. Hails, J. D. Kennedy, and W. S. McDonald, *J. Chem. Soc., Dalton Trans.*, 1985, 953.
17 M. A. Beckett, N. N. Greenwood, J. D. Kennedy, and M. Thornton-Pett, *Polyhedron*, 1985, **4**, 505.
18 X. L. R. Fontaine, H. Fowkes, N. N. Greenwood, J. D. Kennedy, and M. Thornton-Pett, *J. Chem. Soc., Dalton Trans.*, 1986, 547 and refs. therein.
19 J. Bould, J. E. Crook, N. N. Greenwood, and J. D. Kennedy, *J. Chem. Soc., Chem. Commun.*, 1983, 951.
20 J. Bould, N. N. Greenwood, and J. D. Kennedy, *J. Organomet. Chem.*, 1983, **249**, 11.
21 M. Elrington, N. N. Greenwood, J. D. Kennedy, and M. Thornton-Pett, *J. Chem. Soc., Chem. Commun.*, 1984, 1398.
22 S. G. Shore, D-Y. Jan, L-Y. Hsu, and W-L. Hsu, *J. Am. Chem. Soc.*, 1983, **105**, 5923.
23 D. F. Gaines and T. V. Iorns, *Inorg. Chem.*, 1968, **7**, 1041.
24 J. W. Lott and D. F. Gaines, *Inorg. Chem.*, 1974, **13**, 2261.
25 D. F. Gaines and S. J. Hildebrandt, *Inorg. Chem.*, 1978, **17**, 794.
26 F. Klanberg and L. J. Guggenberger, *Chem. Commun.*, 1967, 1293.
27 F. Klanberg, E. L. Muetterties, and L. J. Guggenberger, *Inorg. Chem.*, 1968, **7**, 2272.
28 P. A. Wegner, L. J. Guggenberger, and E. L. Muetterties, *J. Am. Chem. Soc.*, 1970, **92**, 3473.
29 J. R. Moss and B. L. Shaw, *J. Chem. Soc., Dalton Trans.*, 1972, 1910.
30 P. G. Douglas and B. L. Shaw, *Inorg. Synth.*, 1977, **17**, 64.
31 J. Chatt, G. J. Leigh, D. M. P. Mingos, and R. J. Paske, *J. Chem. Soc. A*, 1968, 2636.
32 T. C. Gibb and J. D. Kennedy, *J. Chem. Soc., Faraday Trans. 2*, 1982, 525.
33 S. K. Boocock, Y. M. Cheek, N. N. Greenwood, and J. D. Kennedy, *J. Chem. Soc., Dalton Trans.*, 1981, 1430.
34 A. Modinos and P. Woodward, *J. Chem. Soc., Dalton Trans.*, 1981, 1414.
35 N. Walker and P. Stuart, *Acta Crystallogr., Sect. A*, 1983, **39**, 158.
36 G. M. Sheldrick, SHELX76, Program System for *X*-Ray Structure Determination, University of Cambridge, 1976.

Received 23*rd May* 1985; *Paper* 5/867